Molecular architecture of intermediate filaments

Sergei V. Strelkov,[1]* Harald Herrmann,[2] and Ueli Aebi[1]

Summary

Together with microtubules and actin microfilaments, ~11 nm wide intermediate filaments (IFs) constitute the integrated, dynamic filament network present in the cytoplasm of metazoan cells. This network is critically involved in division, motility and other cellular processes. While the structures of microtubules and microfilaments are known in atomic detail, IF architecture is presently much less understood. The elementary 'building block' of IFs is a highly elongated, rod-like dimer based on an α-helical coiled-coil structure. Assembly of cytoplasmic IF proteins, such as vimentin, begins with a lateral association of dimers into tetramers and gradually into the so-called unit-length filaments (ULFs). Subsequently ULFs start to anneal longitudinally, ultimately yielding mature IFs after a compaction step. For nuclear lamins, however, assembly starts with a head-to-tail association of dimers. Recently, X-ray crystallographic data were obtained for several fragments of the vimentin dimer. Based on the dimer structure, molecular models of the tetramer and the entire filament are now a possibility. ***BioEssays*** **25:243–251, 2003.**

Introduction

The cytoskeleton of all metazoan cells contains three major filament systems: actin microfilaments (MFs), microtubules (MTs) and intermediate filaments (IFs).[1–3] The name 'intermediate filaments' comes from their diameter (10–12 nm) being intermediate between that of MTs (25 nm) and MFs (7–10 nm). The integrated network formed by the three filament systems is responsible for the mechanical integrity of the cell and is critically involved in such processes as cell division, motility and plasticity. IF proteins (lamins) are also found in the cell nucleus, forming a meshwork of filaments on the inside of the nuclear membrane. In vivo, IFs function in close interaction with associated cytoskeletal components such as motor proteins and plakin-type cross-bridging proteins.[4,5]

IFs exhibit unique structural features clearly differentiating them from two other filament systems. Firstly, the elementary 'building blocks' of both MFs and MTs are represented by globular proteins, a monomeric actin and an αβ-tubulin heterodimer, respectively. However, the elementary unit of IFs is a very elongated (~45 nm) and thin (~2–3 nm) rod-like dimer. The axes of the elementary dimers are aligned approximately parallel to the filament axis, while the filament width is controlled by a specific lateral association of the dimers. Secondly, both actin MFs and MTs are polar, which allows an active transport of associated motor proteins, such as myosins and kinesins, along these filaments. On the contrary, assembled IFs have no polarity, as individual dimers are oriented in both 'up' an 'down' directions along the filament. Thirdly, in vivo IFs appear to be the most dynamic of the three filament types. In particular, reversible dissociation–association of IF dimers can occur along the entire filament length and not just at the two ends as in MTs and MFs.

At present, IFs are the least characterised structurally of the three filament systems. The crystal structure of globular actin[6,7] as well as that of the tubulin dimer[8,9] have been determined, and the respective filaments were extensively studied by electron microscopy (EM). It was established that the arrangement of monomers in either case follows a helical symmetry. By fitting the crystal structures into the corresponding three-dimensional EM reconstructions, atomic models for both MTs and MFs could be built. At the same time, our current knowledge of IF structure is considerable only at the level of elementary dimers, as will be discussed. Our understanding at the level of mature IFs is very far from being complete, and there is still no consensus on the exact arrangement of the dimers within the filament.

Structural information at atomic resolution is indispensable for the understanding of IF function in the living cell. Most importantly, it can provide clues to the mechanism of various human diseases caused by mutations in IF proteins, such as keratins, desmin or nuclear lamins.[2,10,11] It was shown that

[1]Maurice E. Müller Institute for Structural Biology, Biozentrum Basel, Switzerland.
[2]German Cancer Research Centre, Heidelberg, Germany.
Funding agencies: The Deutsche Forschungsgemeinschaft (grant: HE 1853 to H.H.), The Swiss National Science Foundation (to U.A.), Canton Basel-Stadt and the M.E. Müller Foundation of Switzerland.
*Correspondence to: Sergei V. Strelkov, M. E. Müller Institute for Structural Biology, Biozentrum, University of Basel, Klingelbergstrasse 70, CH-4056 Basel, Switzerland. E-mail: sergei-v.strelkov@unibas.ch
DOI 10.1002/bies.10246
Published online in Wiley InterScience (www.interscience.wiley.com).

Abbreviations: IF, intermediate filament; ULF, unit-length filament; MF, microfilament; MT, microtubule; EM, electron microscopy; NMR, nuclear magnetic resonance; AFM, atomic force microscopy.

such diseases are often due to single amino-acid replacements that nevertheless drastically affect IF assembly and function. In this short essay, we will focus on the most recent advances towards understanding of IF architecture, including the first crystallographic X-ray data on IF dimer.

Primary sequence of IFs

IF proteins are differentially expressed in most tissues and cell types. 65 human IF genes, as well as their orthologs in numerous other species, have been identified and sequenced.[12–14] All IF proteins exhibit a characteristic 'tripartite' structure (Fig. 1A), which includes the highly α-helical central domain, the 'rod', and the non-helical 'head' and 'tail' domains located at either end of the rod domain.[2,15] Cytoplasmic IF proteins can be classified into four major types according to their sequence simularity, while the fifth type represents the nuclear lamins. Fig. 1B shows the sequence alignment of the rod domains of human epidermal cytokeratin 18 (type I IF protein), cytokeratin 8 (type II), vimentin (type III), neurofilament L protein (type IV) and nuclear lamin A (type V).

The central rod domain reveals a pronounced seven-residue periodicity, $(abcdefg)_n$, in the distribution of apolar residues. Within this repeat, positions *a* and *d* are preferentially occupied by small apolar residues like Leu, Ile, Met or Val (see Fig. 1B). Such heptad repeat is a 'signature' of a so-called coiled-coil structure. A coiled coil is formed by two or more α-helices wound around each other in a 'superhelix', and constitutes a widespread structural motif in proteins.[16,17] Coiled coils were discovered half a century ago by X-ray diffraction on hair and quill, which contain highly oriented fibres of α-keratin Ifs.[18] Hence it was an IF protein where coiled coils were first found.

The coiled-coil structure defines the overall elongated shape of IF dimer. The heptad periodicity within the rod domain is interrupted in several places, which generates four consecutive α-helical segments: 1A and 1B, which together form the so-called coil 1, and 2A and 2B, which form coil 2 (Fig. 1A,B). The four α-helical segments are interconnected by relatively short, variable linkers L1, L12 and L2. In vertebrate cytoplasmic IF proteins, the central rod domain contains close to 310 residues and the lengths of the individual α-helical

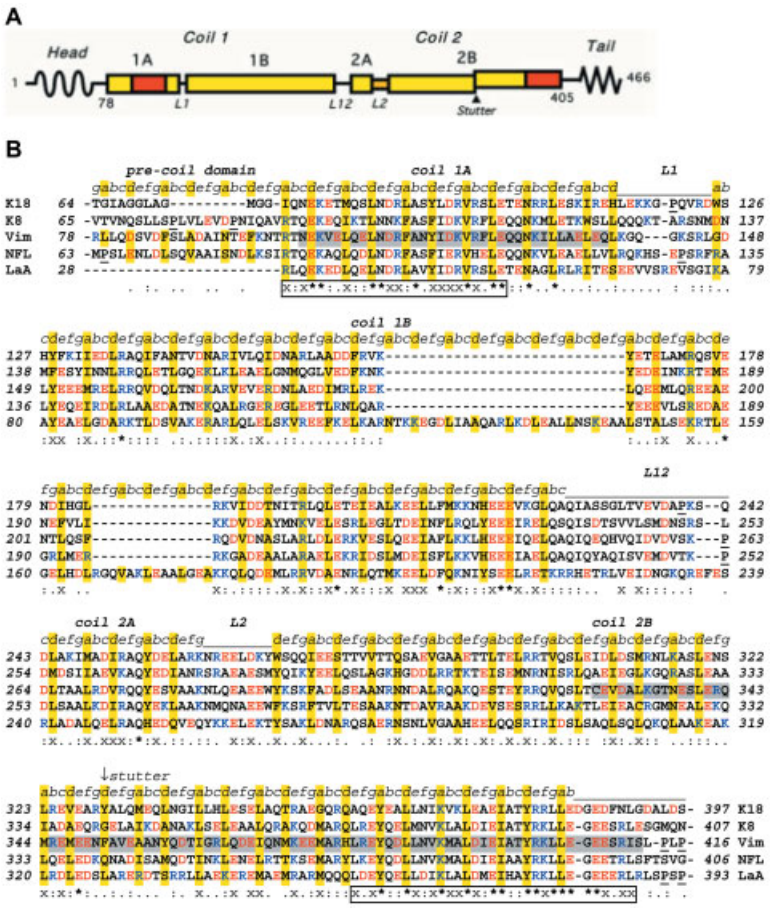

Figure 1. Primary structure of IF proteins. **A:** Schematic diagram of human vimentin. Rectangles show α-helical segments. The two highly conserved regions are highlighted in red. The relatively rigid linker L2[29] is depicted by a small hatched box. **B:** Amino-acid sequence alignment of the rod domains of human IF proteins including cytokeratins 18 and 8, vimentin, neurofilament L protein and nuclear lamin A. The heptad repeats are marked as *abcdefg*, with core positions highlighted with yellow. Basic and acidic residues are shown in blue and red, respectively. The shaded regions of the vimentin sequence have been resolved crystallographically. The line below the alignment shows the sequence similarity score *s* of a particular residue in the seven proteins: '*', $s = 1.0$ (absolutely conserved); 'x', $0.75 \leq s < 1.0$; ':', $0.5 \leq s < 0.75$; '.', $0.25 \leq s < 0.5$ (see Ref. 21 for details). The two most conserved regions are shown in boxes.

segments are absolutely conserved.[2,11] However, the segment 1B of both nuclear lamins and invertebrate IF proteins is by six heptads longer than that of the other IFs (Fig. 1B). Interestingly, apart from the IF rod, such a segmented structure is found in the triple-stranded coiled coil of bacteriophage T4 fibritin,[19] which consists of 13 interconnected segments.

The sequence conservation across different IF proteins is especially pronounced within two regions that are located at either end of the coiled-coil rod (Fig. 1B). The first conserved region spans 26 residues corresponding to about 2/3 of the α-helical segment 1A, while the second conserved region (32 residues) is situated at the very end of the 2B segment. Both of these conserved regions are critically involved in specific dimer–dimer interactions within the mature filament as will be discussed below. Another highly conserved feature of the IF rod is a discontinuity in the heptad repeat pattern within segment 2B, a so-called 'stutter'.[20,21] A stutter is equivalent to an insertion of four extra residues into a continuous heptad repeat. The stutter occurs in exactly the same position, roughly in the middle of segment 2B in all IF proteins[22] (Fig. 1B).

Most IF proteins assemble into homodimers but keratins are obligatory heterodimers formed by one acidic chain (such as cytokeratin 18) and one basic or neutral chain (such as cytokeratin 8). In addition, certain IF proteins, even those belonging to different sequence homology types, can form heterodimers with each other. Correspondingly, three assembly groups of IF proteins exist (Table 1). The first assembly group comprises keratins and the second most other cytoplasmic IFs. The third group includes the nuclear lamins, which apparently do not copolymerise with other vertebrate IFs because of the longer 1B segment.

Finally, the head and tail domains vary considerably in both length and sequence among different IF proteins.[23,24] It is due to the variability of the end domains that IF proteins exhibit a wide range of sizes: for instance, vimentin is a relatively small IF protein with a molecular weight of 55 kDa, whereas neurofilament H protein is longer with a molecular weight of 130 kDa. At the same time, both the tail and especially the head domain are important for the correct filament assembly.

Table 1. Classification of Vertebrate IF Proteins

Localisation	Assembly group	Chain type	Examples
Cytoplasm	1	I	Acidic keratins (pI ~ 4.9–5.7)
		II	Basic keratins (pI ~ 6.1–7.8)
	2	III	Vimentin, desmin, glial fibrillary acidic protein (GFAP), peripherin
		IV	Neurofilament proteins (NF-L, NF-M, NF-H), internexin
Cell nucleus	3	V	Lamins
Eye lens cells (cytoplasm)	?	?	Phakinin, filensin

Structure of the elementary IF dimer

During the last three years, first X-ray crystallographic data on the vimentin rod domain have become available.[21,25,26] Obtaining three-dimensional crystals of any IF component has long been a major challenge, as the highly elongated full-length IF dimers spontaneously assemble into filaments and hence are poorly suited for crystallisation. To overcome this, a 'divide-and-conquer' approach was employed.[26] This approach is based on analysing multiple, relatively short fragments (37 to about 100 residues in length) produced using recombinant techniques. Several of these fragments yielded well-diffracting crystals that could be used for structure determination. Until now, atomic structures at resolutions between 1.4 and 2.3 Å have been completed for segment 1A (residues 102–138; atomic coordinates are available at the Protein Data Band as entry 1gk7) and for the major part of segment 2B (two overlapping fragments: residues 328–411, entry 1gk4, and residues 385–412, entry 1gk6). Using these structures as well as molecular modelling, an atomic model of the complete vimentin dimer has been constructed (Fig. 2A).[21]

The crystal structure of the vimentin fragment corresponding to segment 1A has revealed a single α-helix.[21] The helix is slightly bent so that the hydrophobic patch formed by side chains in *a* and *d* positions locates on the concave side of the curvature. When two such helices are artificially docked together by their hydrophobic sides, a nearly perfect coiled-coil geometry emerges.[27] This is probably what happens in the full-length protein once the 1A helices are joined together at their C termini by the remainder of the rod (Fig. 2A). However, the coiled coil formed by 1A helices is likely to be only marginally stable due to the destabilisation by two bulky residues, Phe114 and Tyr117, which appear in two consecutive hydrophobic core positions close to the middle of this relatively short segment.[27] It was thus suggested—but not yet confirmed experimentally—that the labile 1A segment might be 'unzipping' at some stages of IF assembly.[21] Such a feature could provide an increased mobility to the head domains, which must interact with specific sites on the adjacent dimers in the complete IF structure (see e.g. Ref. 11).

Crystallographic studies have also provided a detailed structure of the major part of vimentin segment 2B. This segment forms a proper coiled coil terminating with residue Glu405 (Fig. 2B),[21] i.e. one heptad earlier than predicted from the primary sequence.[12] The termination of the coiled coil is apparently mediated by the repulsion between the acidic clusters Glu405-Gly406-Glu407-Glu408 so that the two

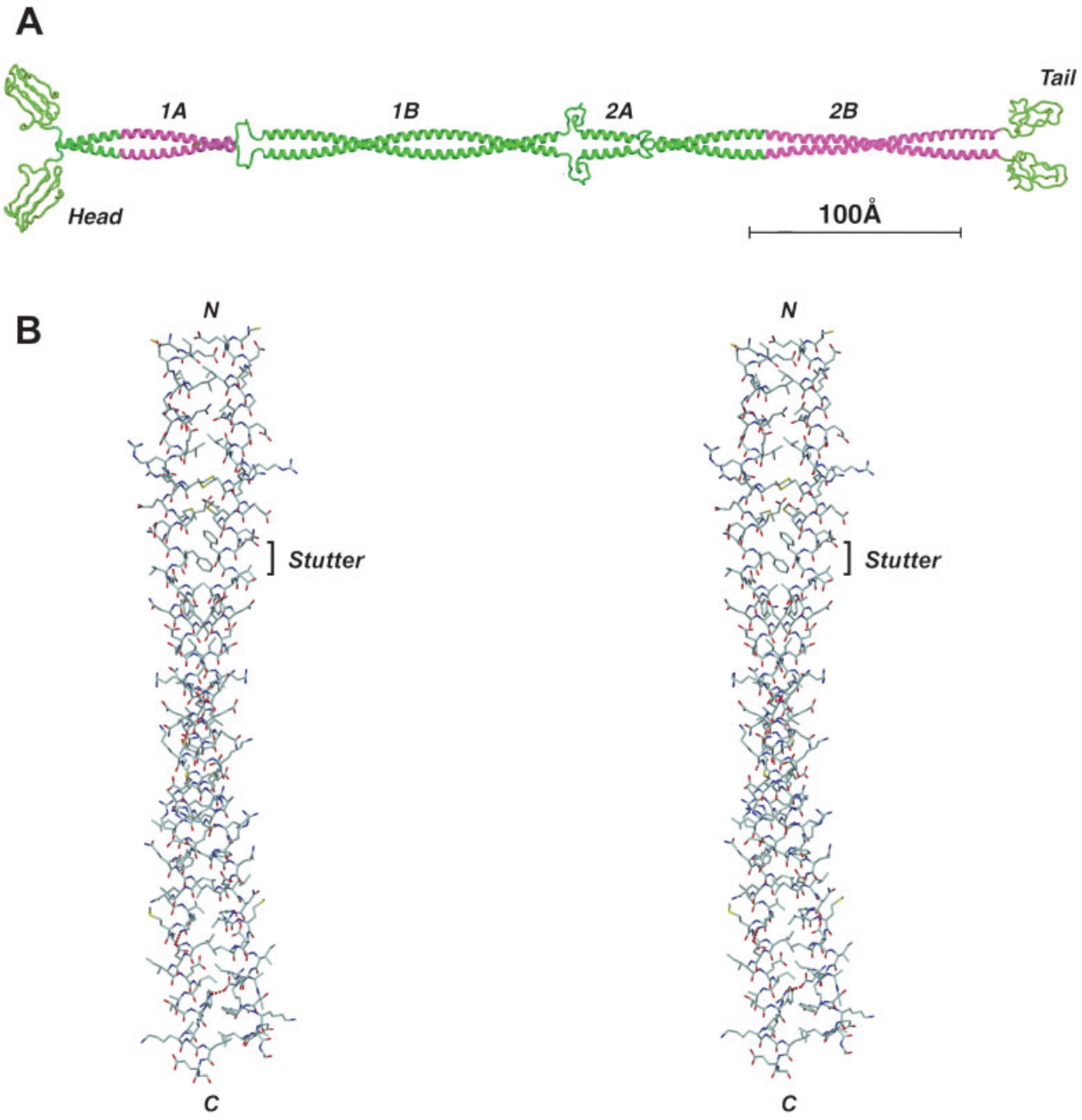

Figure 2. Atomic structure of the vimentin dimer. **A:** Model of the IF dimer.[21] Crystallographically determined regions and modelled regions are shown in magenta and green, respectively. **B:** Crystal structure of the major part of segment 2B (residues 328 to 405) shown in stereo.

chains fold away from the dimer axis. This acidic cluster constitutes the second half of the nearly absolutely conserved *YRKLLEGEE* motif of segment 2B.[25] Moreover, the presence of the heptad stutter at residue Phe351 causes a local unwinding of the otherwise intact coiled coil, so that the two α-helices become nearly parallel[20] (Fig. 2B). This unwinding is apparently required to define the optimal azimuthal orientation of the functionally relevant residues in the N- and C-terminal parts of the rod, respectively, upon IF assembly. Indeed, a 'stutterless' vimentin mutant with an insertion of three residues (i.e., with a continuous heptad repeat throughout the 2B segment) is capable of lateral assembly of dimers but does

not elongate,[28] probably because certain dimer–dimer interactions become altered.

At present, no X-ray structures are available for the three linker regions. However, linker L2 does not include Pro or Gly residues like the two other linkers; in addition, its length is conserved at eight residues in all IF proteins (see Fig. 1B). Accordingly, computer modelling suggested that linker L2 could have a well-defined, relatively rigid conformation.[29] In contrast, linkers L1 and L12 are highly flexible and may serve as 'hinges' between the coiled-coil segments. This might explain the curved appearance of the rod domain on the EM images of individual IF dimers (see for example Ref. 30).

Finally, sequence analyses of IF head domains point to a highly flexible conformation with low content of secondary structure,[11] strongly suggesting that crystallisation of the head domains would be a difficult task. Recently, the globular protease-resistant domain of the lamin tail has been examined by both crystallography and nuclear magnetic resonance spectroscopy (NMR).[31,32] This domain has an immunoglobulin-like fold containing exclusively β-structure. Furthermore, is known that the 'tailless' deletion mutants form IFs with somewhat increased width in vivo and in vitro,[24,33] which indicates that the tail domain is not essential for IF assembly. However, additional structural studies are clearly necessary to obtain a more detailed insight into its functional role.

IF assembly

Tetramer formation is the first assembly step beyond dimers. In fact, tetramers are the smallest soluble oligomers detectable in vivo.[34] Furthermore, the solution of recombinant vimentin in 5 mM Tris-HCl buffer (pH8.4) contains predominantly tetramers.[24] The assembly of vimentin IFs can be readily initiated by increasing the ionic strength of the solution.[28] Within one or two seconds after NaCl addition, rod-like structures with an average length of about 60 nm and a diameter of about 16 nm were observed[24] (Fig. 3A). These distinct structures, termed the unit-length filaments (ULFs), result from a lateral association of dimers. Vimentin ULFs most typically contain 16 dimers but this number may vary depending on the assembly conditions such as pH, ionic strength and temperature.[24,35] Once formed, the ULFs start to anneal longitudinally into extended filaments (Fig. 3B). Subsequently, the filaments undergo some internal rearrangement of subunits leading to a radial compaction.[35] The filament diameter decreases to about 11 nm while their mass-per-length ratio and hence the extension in the longitudinal direction remain unchanged (Fig. 3C).

However, it should be noted that the filament assembly pathways may seriously differ between different IF types and even individual IF proteins. In particular, the longitudinal assembly may proceed concurrently or even prior to the lateral assembly. Correspondingly, the ULF stage characteristic for the type III proteins such as vimentin may be completely missing.[11] For instance, nuclear lamins exhibit a pronounced tendency for a head-to-tail polymerisation of dimers before any significant lateral association occurs.[30] Assembly of invertebrate cytoplasmic IFs proceeds via formation of tetrameric protofilaments (see next section) which then associate laterally.[36]

At present, most conclusions on the specific intermolecular interactions involved in IF assembly are based on examining the effect of certain point mutations or deletions. On one hand, such studies have indicated that the highly conserved regions at either end of the rod domain are critical for the correct assembly.[2,37] On the other hand, it was established that the head domains should play an essential role already at the tetramer stage, as mutant vimentins with sufficiently long N-terminal deletions of the head do not

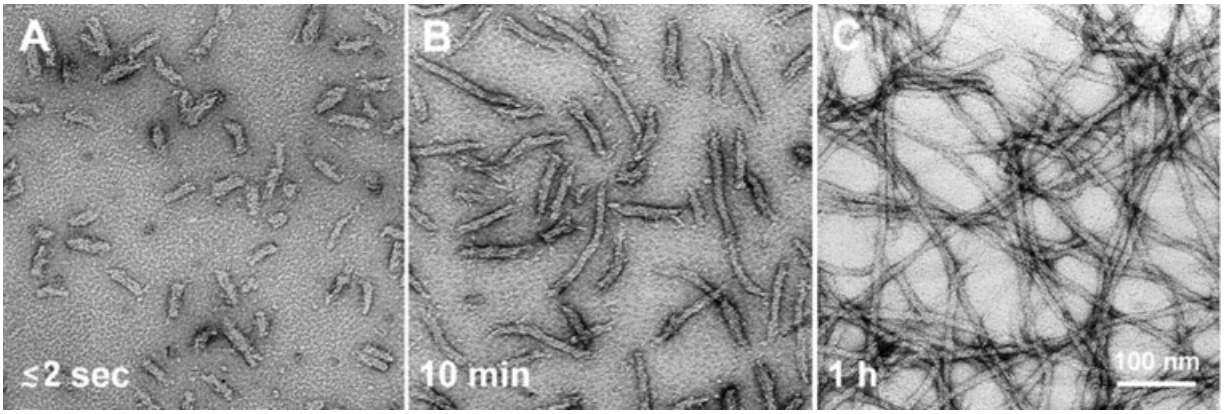

Figure 3. In vitro assembly of recombinant human vimentin. The assembly was initiated by addition of the 'filament buffer' to the final concentration of 25 mM Tris–HCl (pH 7.5) and 50 mM NaCl (see Ref. 28 for details). Negatively stained EM images were taken after (A) 1–2 seconds, (B) 10 minutes and (C) 1 hour of assembly. Scale bar is 100 nm.

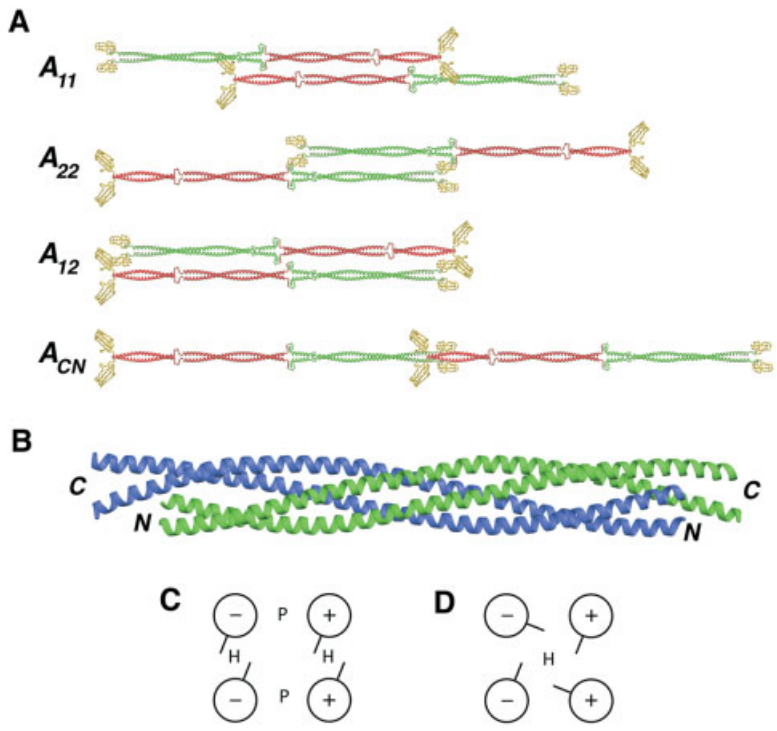

Figure 4. Dimer–dimer association. **A:** Four association modes A_{11}, A_{22}, A_{12} and A_{CN}. Coil 1 and coil 2 are coloured red and green, respectively. **B:** Model for the overlap region of the A_{22} tetramer based on the known atomic structure of segment 2B.[21] The two antiparallel coiled-coil dimers are in blue and green, respectively. **C:** Cross-section of the tetramer model shown above. The two coiled coils are joined together by a predominantly polar interface (P). 'Up' and 'down' orientations of the α-helices are designated by plus and minus signs, respectively. **D:** An alternative model: a four-stranded, antiparallel coiled coil with a common hydrophobic core (H).

assemble beyond dimers (Ref. 24; H. Herrmann et al., unpublished data). In particular, the heads are likely to interact with specific sites on the coiled-coil rod[21] (see also Fig. 4A), but the exact localisation of such sites is not known. An important contribution to this interaction should be provided by electrostatic attraction, as the head domains are very basic due to a high content of arginine residues whereas each of the four coiled-coil segments and also the tail domain are acidic (for instance, the rod domain of human vimentin has a pI of 4.7). In contrast, deletion of the tail domain does not abolish filament formation, but 'tailless' vimentin mutants yielded polymorphic filaments with diameters ranging from normal to 25% increased.[24]

Last but not least, it should be recollected that in vivo IFs are highly dynamic structures. In particular, their interaction with associated proteins apparently requires certain rearrangements within the filament structure.[2,4] This property is also reflected in some interesting in vitro observations: while mature IFs are rather stable thermodynamically (for instance, they do not disassemble in the presence of non-ionic detergents Ref. 38), they readily interact with certain specific peptides, which results in their conversion into aberrant aggregates.[21,39,40]

Dimer–dimer interactions

The lateral association of dimers within IFs is described by three distinct interaction modes denoted A_{11}, A_{22} and A_{12}.[37,41,42] The A_{11} mode corresponds to an antiparallel, half-staggered association of two dimers with their 1B segments approximately aligned (Fig. 4A). It appears that the soluble vimentin tetramers correspond to exclusively A_{11} association, suggesting extensive dimer–dimer contacts in this mode (H. Herrmann et al., unpublished data). Furthermore, the A_{22} mode corresponds to a half-staggered antiparallel association of dimers with the 2B segments aligned, while an unstaggered, antiparallel association of dimers yields the A_{12} mode (Fig. 4A). The staggering of dimers in each mode can be quantified fairly precisely from chemical crosslinking at lysine residues,[42] or by electron paramagnetic resonance spectroscopy with site-directed spin labelling.[43] In addition, most mature IFs reveal an overlap between the N- and C-terminal parts of longitudinally aligned dimers, denoted as the A_{CN} mode (Fig. 4A). The extent of this overlap can be calculated as the difference between the rod length and the axial repeat of the filament known from the X-ray fibre diffraction and EM data.[11] A linear array of tetramers within a mature IF corresponds to a protofilament, i.e. a structure containing two dimers per cross-section. It may be hypothesised that a protofilament is made up by the A_{11}, A_{22} and A_{CN} contacts, while the A_{12} contact only occurs between adjacent protofilaments.[11]

In the absence of any atomic resolution data, the molecular detail of the dimer–dimer association currently remains uncertain. However, the packing of individual dimers within

mature filaments is rather dense, and one should expect the coiled-coil rods to make extensive interactions within the overlapping region in each of the modes A_{11}, A_{22} and A_{12}. It may be hypothesised that the two oppositely oriented, left-handed coiled coils are in turn wound around each other in a left-handed 'superhelix', such as shown in Fig. 4B. The pitch of this superhelix should be close to the pitch of the coiled coil (140–180 Å). Furthermore, two scenarios of the intermolecular interactions within such a tetramer seem to be possible. On one hand, it is feasible that the hydrophobic cores of either dimer are mostly preserved, while the interactions between dimers are mediated by the predominantly polar groups located on the 'outside' of either coiled coil (Fig. 4C). On the other hand, it is also possible that the association of dimers could result, at least in some regions along their length, in a formation of a four-stranded antiparallel coiled coil (Fig. 4D). The latter scenario would require significant rearrangements within the dimers' structures, as a common hydrophobic core has to be created. Such a structure would resemble the four-stranded SNARE complex that has been studied by X-ray crystallography.[44] We note that, like IFs, the SNARE complex exhibits significant stability as well as dynamic association–dissociation capability, which are both essential for its function during membrane fusion.

Towards the IF architecture: current models

In the past, the three-dimensional architecture of mature IFs and their assembly intermediates has been extensively explored by a number of imaging techniques, most prominently EM and X-ray fibre diffraction. However, the structural detail obtained until now has not yet provided a definite explanation on how the individual dimers are arranged within the filament cross-section. Nevertheless, cryo-EM studies of hard α-keratin and other IF proteins could be used to derive their radial density profiles (Fig. 5A).[45] These profiles are compatible with a structure with ~10 nm diameter, which is however not hollow but appears to contain a low-density core with a diameter of ~3 nm. Such structure is also consistent with X-ray diffraction data from hard α-keratin fibres.[11,46]

It may be suggested that the ULFs formed by the type III IF proteins represent circular assemblies (that is, hollow cylinders) of laterally interacting dimers[37] (Fig. 5B). This is the most symmetrical possibility, and hence it should be favoured from a theoretical standpoint. Such cylinders should result from a lattice-like association of dimers governed by the interaction modes A_{11}, A_{22} and A_{12}.[11] Once the ULFs are annealed into an extended filament, its subsequent compaction demands certain rearrangements in the lateral packing of dimers. The structure of mature IFs apparently involves distinct octameric protofibrils (Fig. 5C). The existence of those is supported by the observed quantisation of the mass-per-length ratios in various IFs, with the minimal increment corresponding to eight chains (four dimers), as well as by

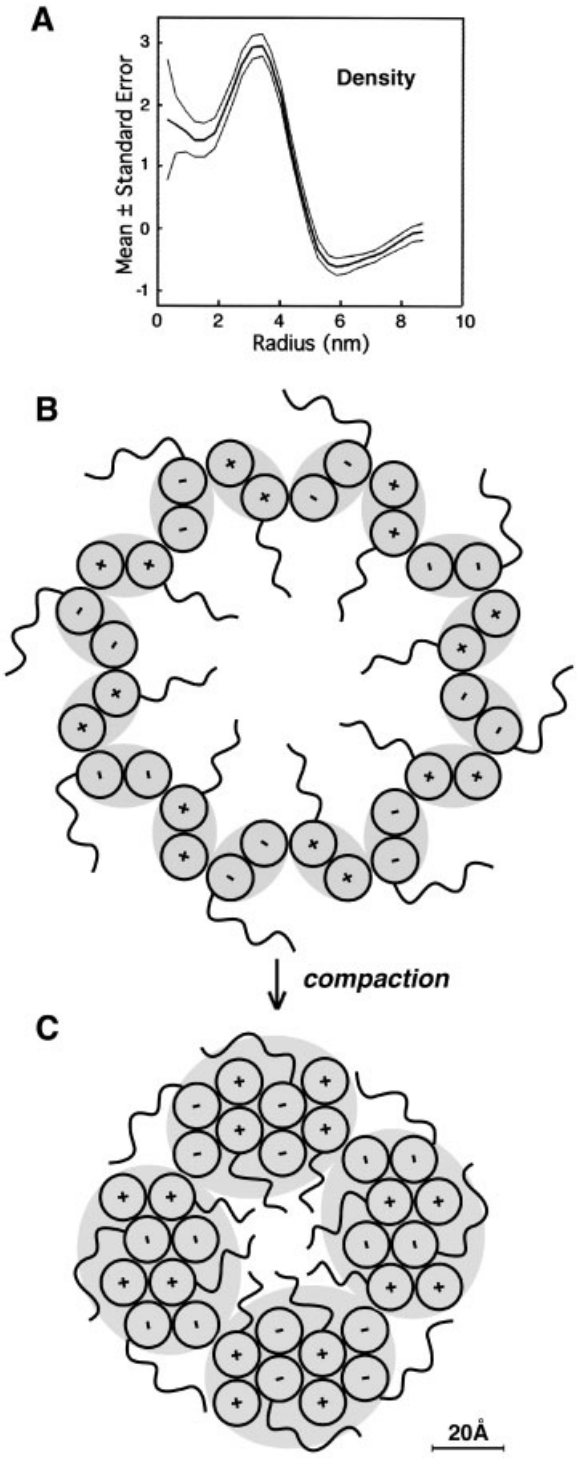

Figure 5. IF architecture. **A:** Experimental radial density distribution of á-keratin IFs. Adapted from Ref. 45. **B:** Schematic model of vimentin ULFs shown as cross-section. Individual dimers are depicted by ovals. **C:** Schematic model of mature vimentin IFs. Four dimers associate into an octamer (shown as a shaded oval), and four octamers constitute the filament.

recent cross-linking data[47] and direct EM observations.[48] Importantly, our schematic structure of mature IFs (Fig. 5C) has the maximal density at a radius of ~35 Å, which is in good agreement with the radial density profiles obtained for hard α-keratin fibres (Fig. 5A). Furthermore, it appears that the 'cylinder' formed by the octamers is somewhat twisted. Indeed, EM images of partially unravelled epidermal keratin IFs reveal a distinct right-handed twisting.[48] Hence it is likely that IFs, like MTs and actin MFs, have a helical symmetry. Finally, the low-density core observed along the filament axis is likely to be formed by the head or/and the tail domains. These domains altogether compose a considerable fraction of the IF dimer mass (~30% in vimentin). At the same time, it is also plausible that some of these domains (for instance, the globular tail domains of lamins) locate on the outside of the structure.

Outlook

Recent X-ray crystallographic studies on vimentin fragments have provided important atomic resolution data on the IF dimer structure (Fig. 2). It is hoped that such data will soon become available for other IF assembly groups as well, particularly nuclear lamins and keratins. Furthermore, it is imperative that atomic detail be obtained on the dimer–dimer interactions at the tetramer level (Fig. 4) and beyond. This can be achieved by the crystallographic studies of stable homotypic and heterotypic complexes formed by certain IF fragments, such as recombinantly expressed lamin 'miniconstructs'[30] or various vimentin fragments.[26] In addition, further three-dimensional reconstructions based on cryo EM studies of complete IFs (either isolated from a natural source or assembled in vitro) and possibly ULFs should also be pursued. Recent technical advances in cryo EM are likely to significantly improve the resolution of such reconstructions. Furthermore, the ultimate conformation of IF chains (including the flexible terminal domains) is very likely to be only achieved within the mature filament once the proper intermolecular contacts are fully established. EM studies at the filament level are thus of great importance towards complementing the atomic resolution data to be obtained by the X-ray and NMR analyses. Finally, the recently introduced atomic force microscopy (AFM) can provide valuable surface topology data on IF architecture. These data are likely to yield further structural detail on the filament packing, supercoiling etc. In addition, AFM can be used to examine the mechanical properties of IFs, such as flexibility.

A full understanding of the IF architecture still remains a challenge. To overcome it, a whole spectrum of experimental approaches, along with the synthetic ability of researchers, have to be pushed to their limits. However, these efforts are likely to pay off, as the knowledge of the IFs' structural principles is indispensable for the understanding of fundamental cellular processes as well as human disease.

Acknowledgments

The authors are most grateful to Drs. Peter Burkhard and Laurent Kreplak for many stimulating discussions and critical reading of the manuscript.

References

1. Schliwa M. The Cytoskeleton Cell Biology Monographs, Vol. 13. 1986. Wien and New York: Springer-Verlag.
2. Fuchs E, Weber K. Intermediate filaments: structure, dynamics, function, and disease. Annu Rev Biochem 1994;63:345–382.
3. Aebi U, Haner M, Troncoso J, Eichner R, Engel A. Unifying principles in intermediate filament structure and assembly. Protoplasma 1988;145: 73–81.
4. Herrmann H, Aebi U. Intermediate filaments and their associates: multitalented structural elements specifying cytoarchitecture and cytodynamics. Curr Opin Cell Biol 2000;12:79–90.
5. Yoon KH, Yoon M, Moir RD, Khuon S, Flitney FW, Goldman RD. Insights into the dynamic properties of keratin intermediate filaments in living epithelial cells. J Cell Biol 2001;153:503–516.
6. Steinmetz MO, Hoenger A, Tittmann P, Fuchs KH, Gross H, Aebi U. An atomic model of crystalline actin tubes: combining electron microscopy with X-ray crystallography. J Mol Biol 1998;278:703–711.
7. Bubb MR, Govindasamy L, Yarmola EG, Vorobiev SM, Almo SC, Somasundaram T, Chapman MS, Agbandje-McKenna M, McKenna R. Polylysine induces an antiparallel actin dimer that nucleates filament assembly: crystal structure at 3.5-A resolution. J Biol Chem 2002;277: 20999–21006.
8. Nogales E, Wolf SG, Downing KH. Structure of the alpha beta tubulin dimer by electron crystallography. Nature 1998;391:199–203.
9. Gigant B, Curmi PA, Martin-Barbey C, Charbaut E, Lachkar S, Lebeau L, Siavoshian S, Sobel A, Knossow M. The 4 A X-ray structure of a tubulin: stathmin-like domain complex. Cell 2000;102:809–816.
10. Fuchs E, Coulombe PA. Of mice and men: genetic skin diseases of keratin. Cell 1992;69:899–902.
11. Parry DAD, Steinert PM. Intermediate filaments: molecular architecture, assembly, dynamics and polymorphism. Q Rev Biophys 1999;32:99–187.
12. Conway JF, Parry DAD. Intermediate filament structure. 3. Analysis of sequence homologies. Int J Biol Macromol 1988;10:79–98.
13. Herrmann H, Aebi U. Structure, assembly, and dynamics of intermediate filaments. Subcell Biochem 1998;31:319–362.
14. Hesse M, Magin TM, Weber K. Genes for intermediate filament proteins and the draft sequence of the human genome: novel keratin genes and a surprisingly high number of pseudogenes related to keratin genes 8 and 18. J Cell Sci 2001;114:2569–2575.
15. Geisler N, Weber K. The amino acid sequence of chicken muscle desmin provides a common structural model for intermediate filament proteins. EMBO J 1982;1:1649–1656.
16. Lupas A. Coiled coils: new structures and new functions. Trends Biochem Sci 1996;21:375–382.
17. Burkhard P, Stetefeld J, Strelkov SV. Coiled coils: a highly versatile protein folding motif. Trends Cell Biol 2001;11:82–88.
18. Crick FHC. Is alpha-keratin a coiled coil? Nature 1952;170:882–883.
19. Tao Y, Strelkov SV, Mesyanzhinov VV, Rossmann MG. Structure of bacteriophage T4 fibritin: a segmented coiled coil and the role of the C-terminal domain. Structure 1997;5:789–798.
20. Strelkov SV, Burkhard P. Analysis of alpha-helical coiled coils with the program TWISTER reveals a structural mechanism for stutter compensation. J Struct Biol 2002;137:54–64.
21. Strelkov SV, Herrmann H, Geisler N, Wedig T, Zimbelmann R, Aebi U, Burkhard P. Conserved segments 1A and 2B of the intermediate filament dimer: their atomic structures and role in filament assembly. EMBO J 2002;21:1255–1266.
22. Weber K, Geisler N. Intermediate filaments: structural conservation and divergence. Ann N Y Acad Sci 1985;455:126–143.
23. Heins S, Aebi U. Making heads and tails of intermediate filament assembly, dynamics and networks. Curr Opin Cell Biol 1994;6:25–33.

24. Herrmann H, Haner M, Brettel M, Muller SA, Goldie KN, Fedtke B, Lustig A, Franke WW, Aebi U. Structure and assembly properties of the intermediate filament protein vimentin: the role of its head, rod and tail domains. J Mol Biol 1996;264:933–953.
25. Herrmann H, et al. The intermediate filament protein consensus motif of helix 2B: its atomic structure and contribution to assembly. J Mol Biol 2000;298:817–832.
26. Strelkov SV, Herrmann H, Geisler N, Lustig A, Ivaninskii S, Zimbelmann R, Burkhard P, Aebi U. Divide-and-conquer crystallographic approach towards an atomic structure of intermediate filaments. J Mol Biol 2001; 306:773–781.
27. Smith TA, Strelkov SV, Burkhard P, Aebi U, Parry DA. Sequence comparisons of intermediate filament chains: evidence of a unique functional/structural role for coiled-coil segment 1A and linker L1. J Struct Biol 2002;137:128–145.
28. Herrmann H, Haner M, Brettel M, Ku NO, Aebi U. Characterization of distinct early assembly units of different intermediate filament proteins. J Mol Biol 1999;286:1403–1420.
29. North AC, Steinert PM, Parry DA. Coiled-coil stutter and link segments in keratin and other intermediate filament molecules: a computer modeling study. Proteins 1994;20:174–184.
30. Stuurman N, Heins S, Aebi U. Nuclear lamins: their structure, assembly, and interactions. J Struct Biol 1998;122:42–66.
31. Dhe-Paganon S, Werner ED, Chi YI, Shoelson SE. Structure of the globular tail of nuclear lamin. J Biol Chem 2002;18:18.
32. Krimm I, Ostlund C, Gilquin B, Couprie J, Hossenlopp P, Mornon JP, Bonne G, Courvalin JC, Worman HJ, Zinn-Justin S. The Ig-like structure of the C-terminal domain of lamin a/c, mutated in muscular dystrophies, cardiomyopathy, and partial lipodystrophy. Structure (Camb) 2002;10: 811–823.
33. Bader BL, Magin TM, Freudenmann M, Stumpp S, Franke WW. Intermediate filaments formed de novo from tail-less cytokeratins in the cytoplasm and in the nucleus. J Cell Biol 1991;115:1293– 1307.
34. Soellner P, Quinlan RA, Franke WW. Identification of a distinct soluble subunit of an intermediate filament protein: tetrameric vimentin from living cells. Proc Natl Acad Sci USA 1985;82:7929–7933.
35. Herrmann H, Aebi U. Intermediate filament assembly: temperature sensitivity and polymorphism. Cell Mol Life Sci 1999;55:1416–1431.
36. Geisler N, Schunemann J, Weber K, Haner M, Aebi U. Assembly and architecture of invertebrate cytoplasmic intermediate filaments reconcile features of vertebrate cytoplasmic and nuclear lamin-type intermediate filaments. J Mol Biol 1998;282:601–617.
37. Herrmann H, Aebi U. Intermediate filament assembly: fibrillogenesis is driven by decisive dimer-dimer interactions. Curr Opin Struct Biol 1998; 8:177–185.
38. Starger JM, Brown WE, Goldman AE, Goldman RD. Biochemical and immunological analysis of rapidly purified 10-nm filaments from baby hamster kidney (BHK-21) cells. J Cell Biol 1978;78:93–109.
39. Hatzfeld M, Weber K. A synthetic peptide representing the consensus sequence motif at the carboxy-terminal end of the rod domain inhibits intermediate filament assembly and disassembles preformed filaments. J Cell Biol 1992;116:157–166.
40. Goldman RD, Khuon S, Chou YH, Opal P, Steinert PM. The function of intermediate filaments in cell shape and cytoskeletal integrity. J Cell Biol 1996;134:971–983.
41. Geisler N, Schunemann J, Weber K. Chemical cross-linking indicates a staggered and antiparallel protofilament of desmin intermediate filaments and characterizes one higher-level complex between protofilaments. Eur J Biochem 1992;206:841–852.
42. Steinert PM, Marekov LN, Parry DA. Diversity of intermediate filament structure. Evidence that the alignment of coiled-coil molecules in vimentin is different from that in keratin intermediate filaments. J Biol Chem 1993;268:24916–24925.
43. Hess JF, Voss JC, FitzGerald PG. Real time observation of coiled-coil domains and subunit assembly in intermediate filaments. J Biol Chem 2002;16:16.
44. Sutton RB, Fasshauer D, Jahn R, Brunger AT. Crystal structure of a SNARE complex involved in synaptic exocytosis at 2.4 A resolution. Nature 1998;395:347–353.
45. Watts NR, Jones LN, Cheng N, Wall JS, Parry DA, Steven AC. Cryo-Electron microscopy of trichocyte (hard alpha-keratin) intermediate filaments reveals a low-density core. J Struct Biol 2002;137:109–118.
46. Briki F, Busson B, Doucet J. Organization of microfibrils in keratin fibers studied by X-ray scattering modelling using the paracrystal concept. Biochim Biophys Acta 1998;1429:57–68.
47. Parry DA, Marekov LN, Steinert PM. Subfilamentous profibril structures in fibrous proteins. J Biol Chem 2002;276:39253–39258.
48. Aebi U, Fowler WE, Rew P, Sun TT. The fibrillar substructure of keratin filaments unraveled. J Cell Biol 1983;97:1131–1143.